

Charged Particle Identification in CLAS

L. Elouadrhiri

Christopher Newport University, Newport News, Va.

and

Thomas Jefferson National Accelerator Facility, Newport News, Va

V. Burkert, S. Stepanyan

Thomas Jefferson National Accelerator Facility, Newport News, Va.

H. Egiyan

College of William and Mary, Williamsburg, Va

Contents

1	Introduction	2
2	The CEBAF beam RF structure	2
3	The calibration procedure	2
4	Charged particle identification	5
4.1	Pion - Proton separation	5
4.2	Pion-Kaon Separation	5
4.3	Pion - Electron Separation	8
4.4	Missing particle identification	9
4.5	Nuclear target fragments	9
5	Conclusions	10

Abstract

We describe the concept and results of a calibration procedure for the CLAS time-of-flight counters (TOF) with the goal of optimizing charged particle identification in CLAS. We determine the 288 constants needed to tune all TOF strips with respect to the electron beam radiofrequency structure. In this note we describe the method and present results. The method was developed by several of us, and was described in two CALCOM meetings [1]. We show that all charged particles pions, kaons, protons, deuterons, tritons can be separated in the momentum range as covered by the 2.445 GeV runs taken in December 1997. At momenta below about 400 MeV/c one begins to resolve positrons from pions.

1 Introduction

Particle identification in CLAS relies heavily on the combination of measured charged particle momentum and the flight time of the particle from the target to the respective plastic scintillation counters. Other charged particle identification capabilities are due to the gas Cherenkov counters which separate electrons from pions for momenta up to about 3GeV/c, and the energy loss of charged particles in the TOF counters versus particle momentum. Neutral particles (photons and neutrons) identification makes use of timing information of the forward angle and large angle calorimeters. Limited photon-neutron separation is provided by the TOF scintillators to the extent that photons convert with a probability of about 10% in the plastic material, and neutrons interact to about 5% in the same material.

Here we focus on charged particle identification using timing in the TOF counters and particle momenta measured in the CLAS magnet/tracking system. As the procedure makes use of the CEBAF accelerator RF structure we briefly describe this here.

2 The CEBAF beam RF structure

The CEBAF accelerator is based on superconducting accelerating cavities which are operated at a highly stabilized frequency of $1.497 \times 10^9 \text{ sec}^{-1}$. Electrons ride on the crest of the RF field wave with a bunch length of a few picoseconds. Every 3rd bunch of electrons is directed towards one of the 3 experimental areas, creating a train of electrons equally spaced by 2.004nsec. The bunch-to-bunch difference in the beam arriving in the experimental hall is large enough so that it can be resolved by the CLAS time-of-flight counters using scattered electrons. We note that the beam RF structure has previously been used by the CLAS Saclay group to calibrate the photon tagger system [2].

3 The calibration procedure

The TOF counters have photomultiplier readout at both ends of each scintillator strips. The PMT signals are split and brought to Fastbus ADCs and TDCs (latter one after the signal has been discriminated in a timing discriminator (LeCroy 2313)). We assume that the left/right PMT gain matching as well as TDC calibration and time-walk corrections have been carried out with adequate accuracy in an independent procedure [3].

The accelerator RF signal is prescaled by a factor of 40 to provide a signal every 80.16nsec which is then fed into a Fastbus TDC. The TDCs are used in common start mode. They are started by the trigger timing signal and stopped by the RF signal and the detector signals, respectively.

Although the TDCs have been calibrated using a calibration pulser, the RF can be used to check the TDC calibration. For this, we select electrons in any of the scintillator

strips with their known $\beta = 1$ and reconstructed pathlength to correct for flight time differences from the target. Any miscalibration will result in an irregular pattern or even in a complete absence of the "picket fence" structure (Fig. 1).

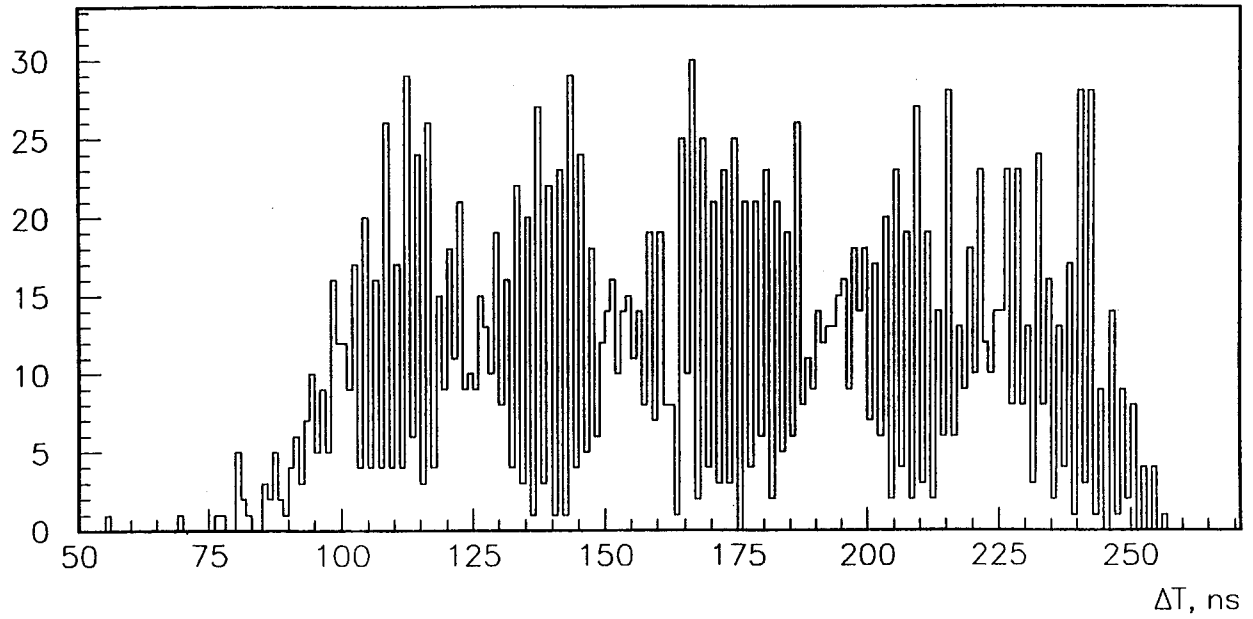


Figure 1: The beam RF structure as seen in the difference of electron start time and RF time when the RF TDC is slightly miscalibrated.

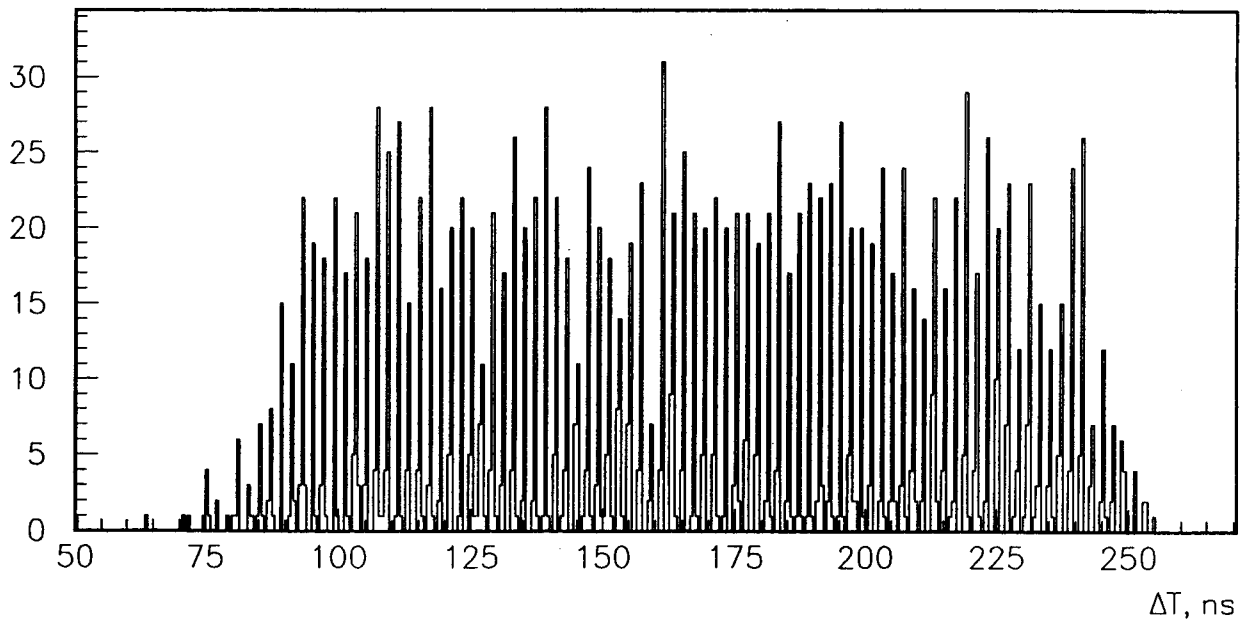


Figure 2: The RF beam structure as seen in the difference of electron start time and RF time. The widths of the peaks is due to the finite resolution of the TOF strips

Since the TDCs are quite linear, a simple adjustment of the number of channels per nsec will usually be sufficient for a uniform structure to emerge. This corrected electron start time is subtracted from RF signal. If the calibration is done correctly the resulting signal will show the RF time structure with its precise spacing of 2.004nsec (Fig. 2).

The calibration procedure was divided into three steps. In the first two steps, only 10 forward SC strips in each sector were considered. First, using the electrons, time differences between that strips and the RF were adjusted to be multiples of RF structure (2.004ns), e.g. the mean of the remainder of the differences to the RF signal was determined:

$$\delta t = AMOD(t_{SC} - t_{TOF} - t_{RF}, RF_{strc}) - RF_{strc}/2.$$

In Fig.3 a typical δt distribution is shown. The observed distributions are fitted to a gaussian function. The fitted mean values are taken as a correction to the strip time.

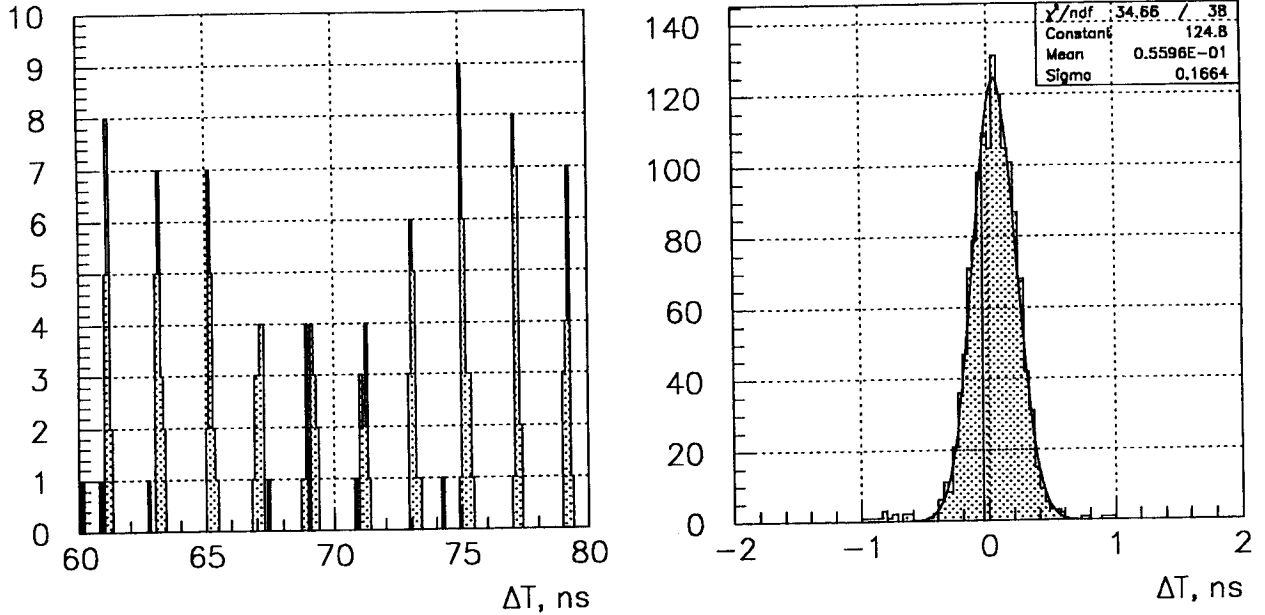


Figure 3: Left side shows $T_{\sigma}T_{RF}$ for one strip. The right hand graph shows $Mod(T - T_{RF}, 2.004)$; the deviation of the mean value from zero shows by how much this particular strip has to be corrected so that only ambiguities of multiples of 2.004nsec remain.

After δt corrections were made to each strip, the time misalignments between the first 10 strips became multiples of 2.004ns.

In order to correct for these differences $e^{-}\pi^{+}$ coincidence events were used. Both electrons and pions were detected in the forward 10 strips in different or in the same sectors. Pions were selected using $\delta E/\delta X$ in SC strips. Time difference between the start times calculated from electron and pion times were analysed:

$$\Delta T = (t_{elSC} - t_{elTOF}) - (t_{piSC} - t_{piTOF})$$

Since at this point gross misalignments are exactly multiples of RF structure (2.004ns), only few tens of events in each coincidence bin are needed to determine the mean values of the time differences.

In the final step the remaining time-of-flight scintillators (11-48 in each sector) were aligned with respect to the 10 forward strips using the same $e^- \pi^+$ events. Electrons were detected in the forward 10 strips, pions in the strips 11 to 48. Time differences ΔT were determined for each remaining strip.

The entire procedure is automated and being run within a PAW session. But still it is highly recommended to check the quality of the fits of the fine tuning with respect to the RF (step 1) by inspecting the histograms and checking the distributions and fit results for the strips that look too noisy and have wider than usual time distributions.

In the following section we apply the calibrated TOF strips in the charged particle identification which employs information from the TOF timing as well as the particle momentum obtained from the tracking in the CLAS magnetic field.

4 Charged particle identification

4.1 Pion - Proton separation

The bulk of particles reconstructed in CLAS will be charged pions and protons. At 4 GeV beam energy pion momenta up to 3 GeV/c are kinematically allowed. In Fig. 4 we show the distribution of masses for all reconstructed hadrons without any kinematical cuts (other than the ones provided by CLAS acceptances) for a 2.445GeV data run. A very clean separation of pions and protons can be seen. On a logarithmic scale the small number of produced K^+ also becomes visible.

The mass peaks cannot be fitted with a single gaussian as they contain a large range of particle momenta. However, a fit to the tip of the peak gives a resolution of about 19MeV for the pions and 24MeV for protons. The calibration procedure makes sure that reconstructed masses and particle momenta are decoupled. This ensures that the ultimate resolution can be achieved. Any correlation between mass and momentum would indicate a flaw in the timing calibration or in the momentum reconstruction.

4.2 Pion-Kaon Separation

In Fig.5 kaons sit on top of a significant tail of background from the huge pion peak. However, kaon identification can be improved if one makes use of kinematical and physics constraints. First, kaons can only be produced above a W of 1.44GeV. In addition, they are produced in association with a strange baryon of at least the mass of the $\Lambda(1115)$. We require $W > 1.65$ GeV to reduce pion contamination to the kaon sample. The results are shown in Fig. 6. The signal/background ratio is significantly improved compared to Fig. 5.

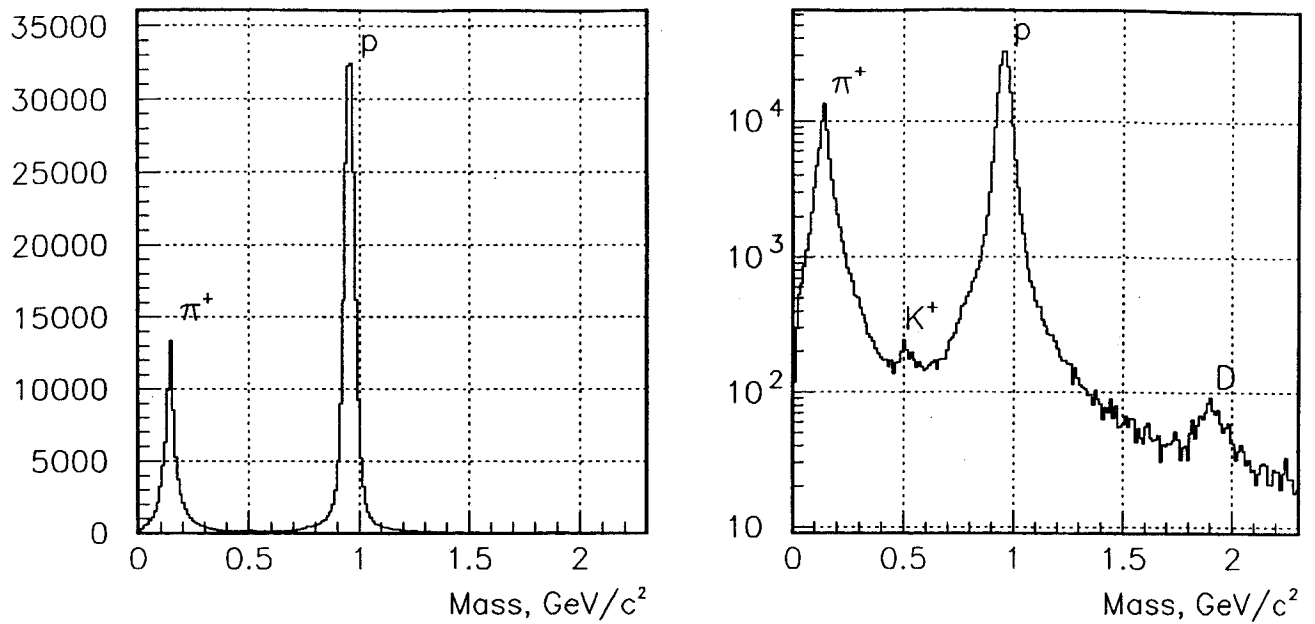


Figure 4: Particle masses as reconstructed from momentum and time-of-flight. All TOF strips and all momenta are included in this graphs.

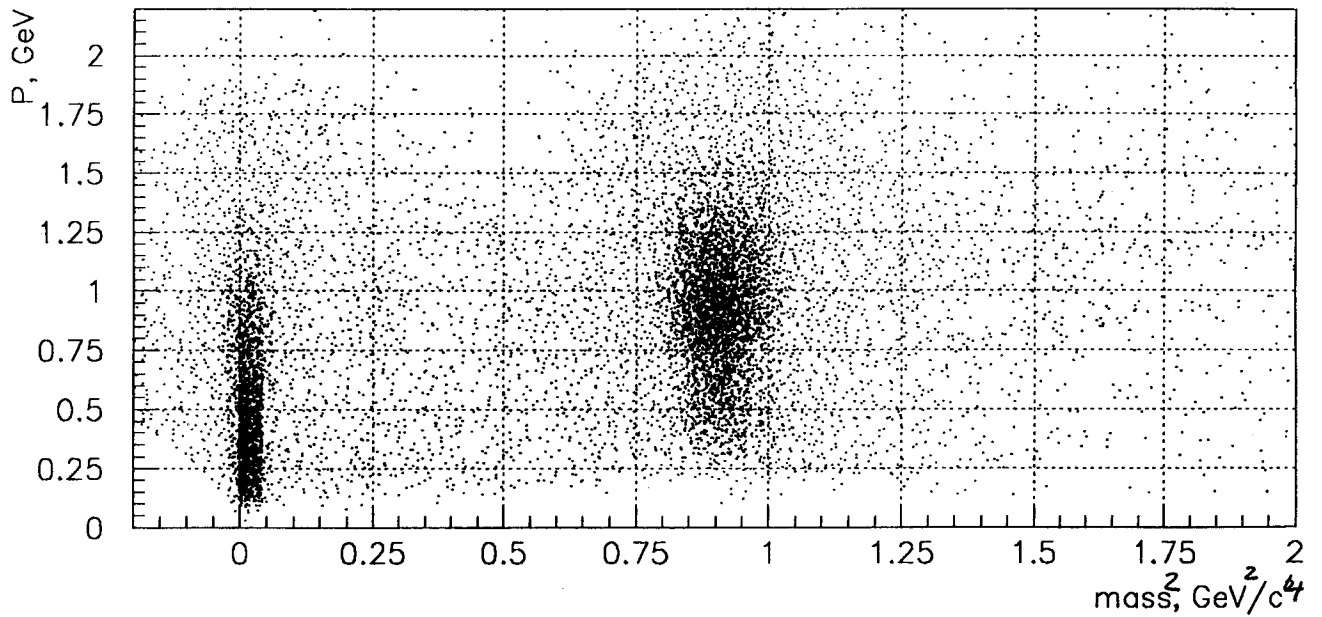


Figure 5: Reconstructed particle masses² versus track momentum . The graph on the left hand shows that the width of the pion mass peak increases with increasing momentum.

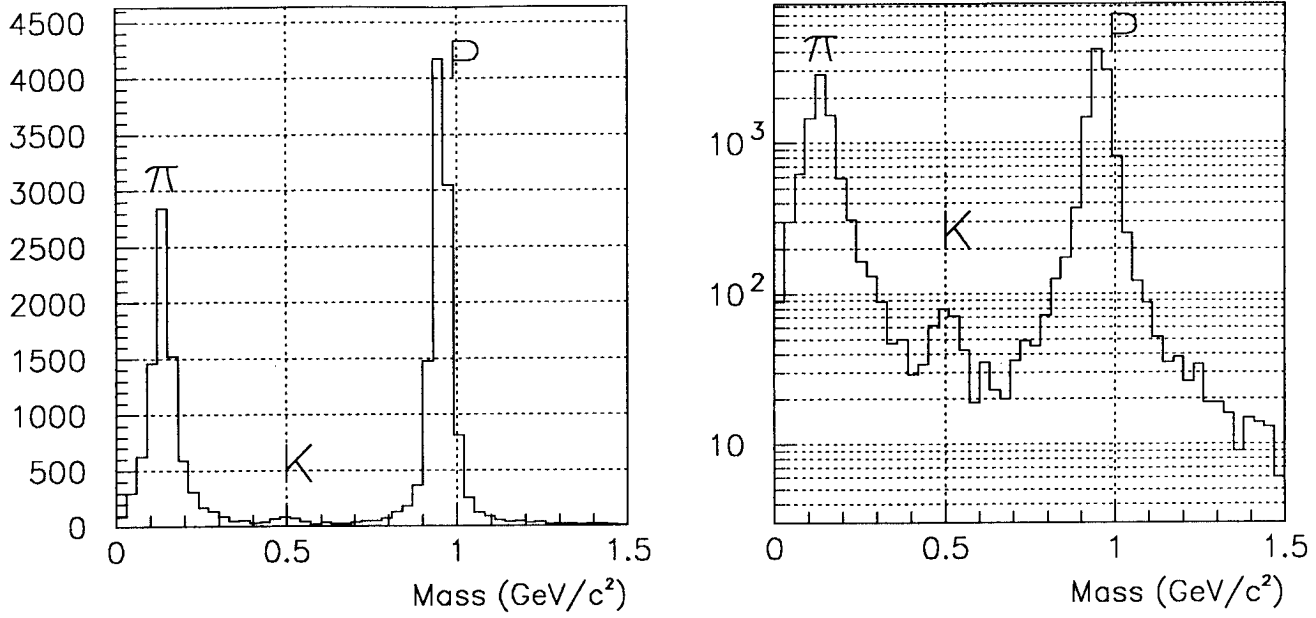


Figure 6: Reconstructed hadron masses for $W > 1.65\text{GeV}$.

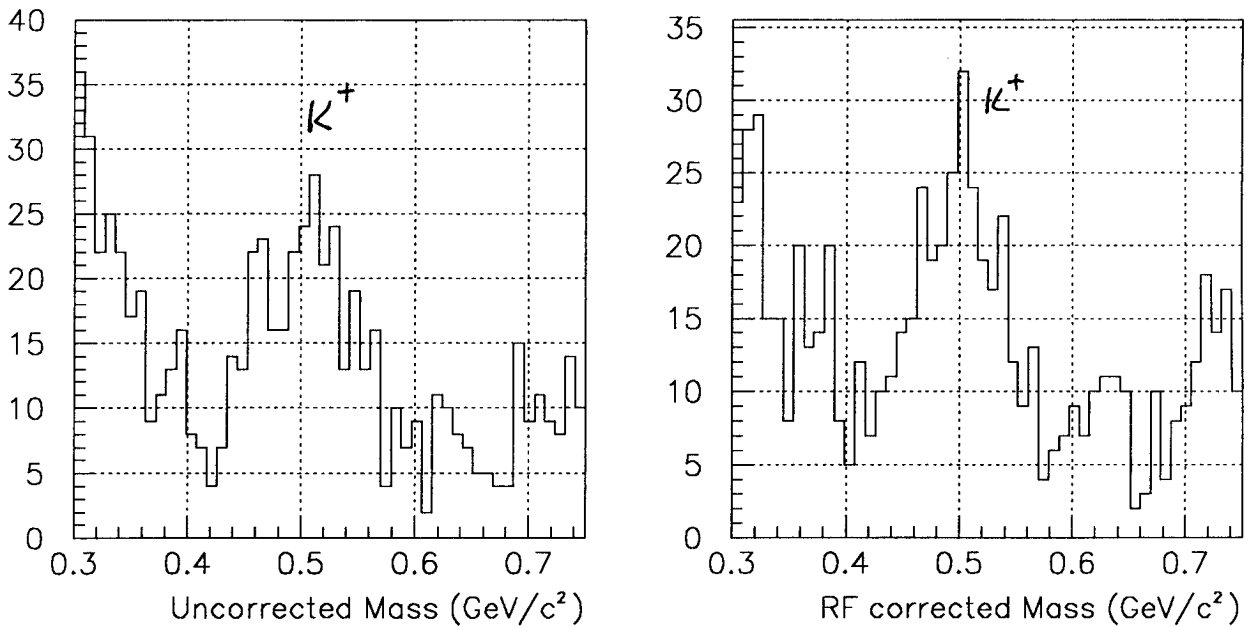


Figure 7: Reconstructed hadron masses in the kaon mass region without and with the RF correction.

Excellent timing resolution is especially important for the identification of kaons at high momenta. In order to achieve this we eliminate the electron contribution to the time resolution by using the RF time rather than the time measured in the scintillators. If both, electrons and hadron would contribute equally to the mass resolution a factor of $\sqrt{2}$ improvement would be achieved. However, electrons are typically detected in shorter scintillator strips with better time resolution than pions. The expected effect is therefore smaller. Figure 7 shows the effect on the kaon mass peak if the RF correction is done. An improvement is visible, indicating that other contributions to the resolution are already sufficiently eliminated to show the effect of the RF timing.

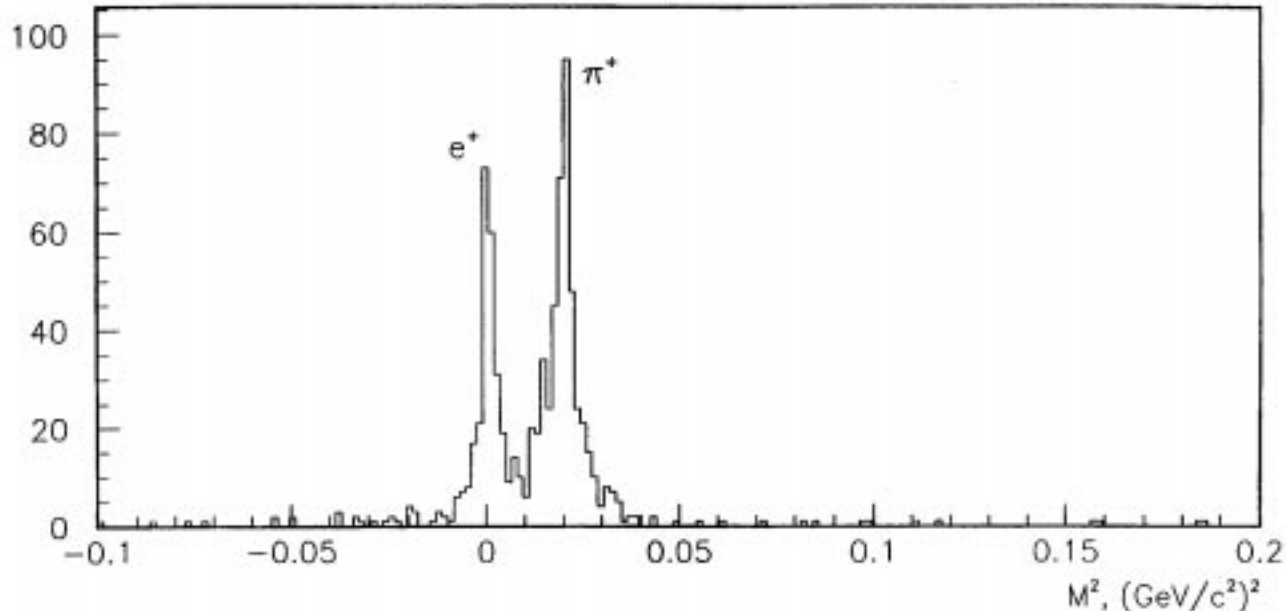


Figure 8: Reconstructed positive particle masses for momenta less than 400MeV/c, and when the positive track is in the same sector as the electron.

4.3 Pion - Electron Separation

Sometimes an event with an electron may also contain a positron. The most likely origin of these events is the conversion of high energy photons into e^+e^- pairs by interacting with the massive structures present in the CLAS detector. These pairs would typically be in the same sector of CLAS.

As these events contribute to the background it is important that they are not misidentified as $e^- \pi^+$ events.

Figure 8 shows the reconstructed mass spectrum for $e^- h^+$ events where both particles are in the same sector, clearly revealing a two-peak structure for the lower momentum bins. One of the peaks is at the pion mass the second one is at $m = 0$, therefore consistent with a positron. The graphs also show that most of the positrons appear at lower masses where they can be separated from pions.

4.4 Missing particle identification

Using the identification of charged particle with the described method will also allow a much improved identification of the non-detected particle. We illustrate this at the example of the $\Lambda(1115)$ and $\Sigma^0(1190)$ which are produced in associate production with K^+ in $ep \rightarrow eK^+\Lambda$, and $ep \rightarrow eK^+\Sigma^0$. Using a mass cut in Figure 7 with $0.45 < m < 0.55$ GeV/c, we calculate the missing mass M_X in $ep \rightarrow eK^+X$, and obtain the results shown in Figure 9, clearly showing the Λ and Σ .

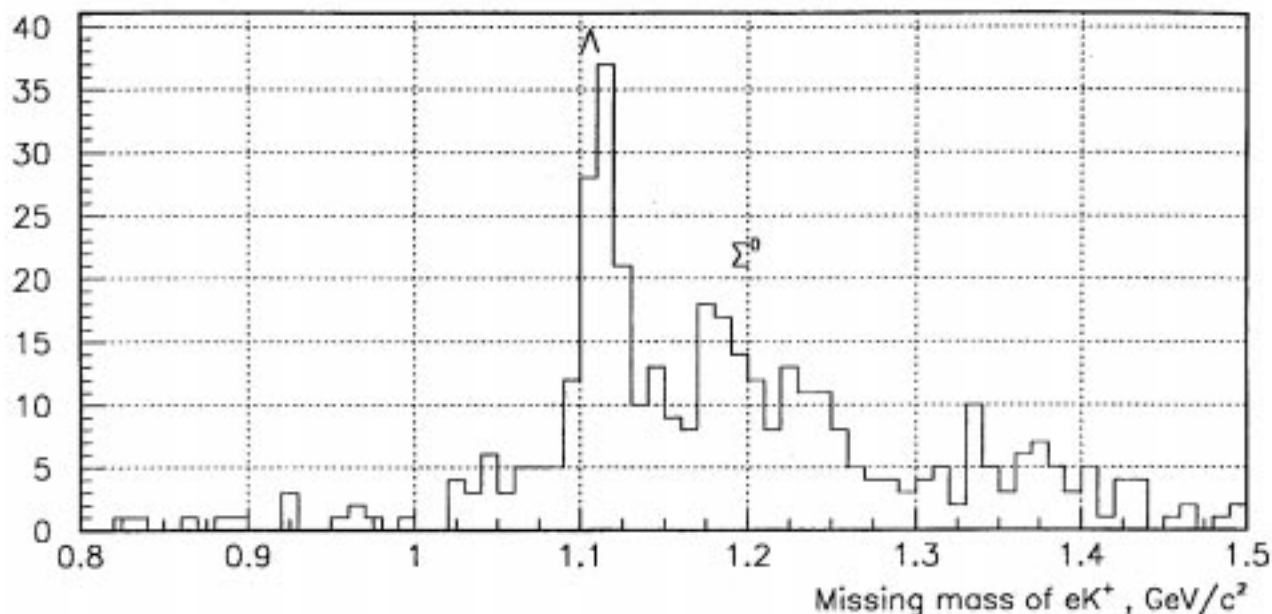


Figure 9: Missing mass distribution for $ep \rightarrow eK^+X$.

4.5 Nuclear target fragments

It is amusing that the mass spectrum also shows nuclear fragments such as deuterons and tritons from the aluminum windows of the liquid hydrogen target cell (Fig. 10). The nuclear components become, of course, much more visible for those runs with empty cells (Fig. 11).

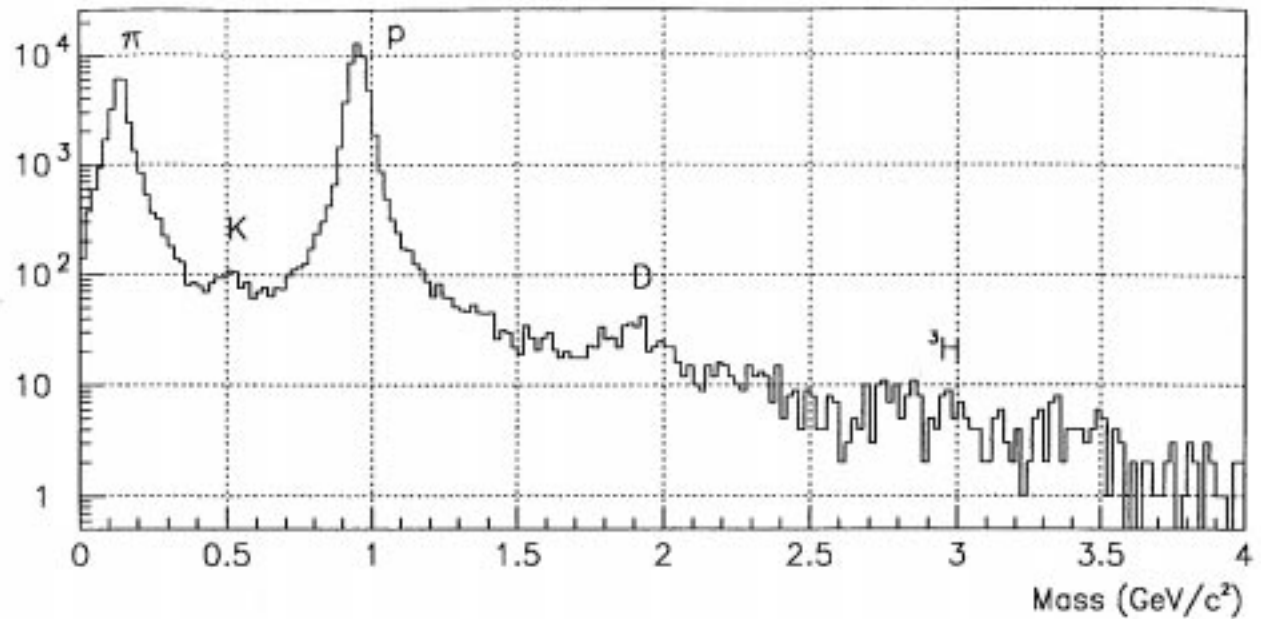


Figure 10: Charged particle showing the full mass spectrum. The heavier fragments are deuterons and tritons, which come from the target cell windows.

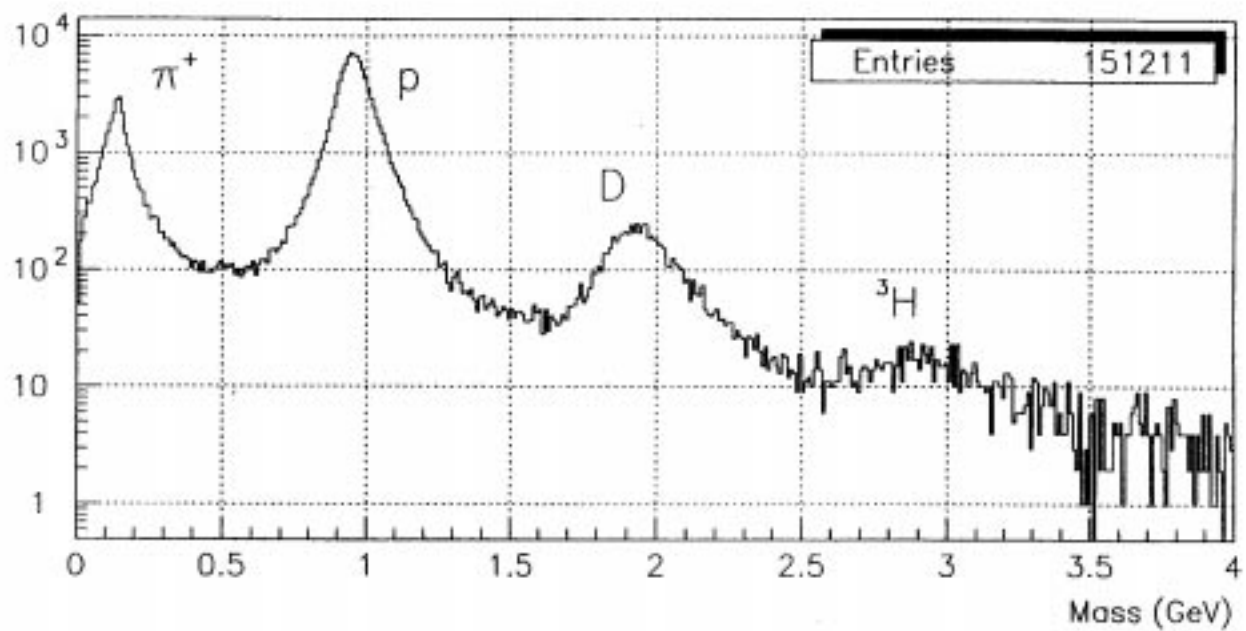


Figure 11: Same as Fig. 10 but with empty target cell.

5 Conclusions

We have outlined a method that provides an accurate and systematic approach to the time calibration of all 288 CLAS TOF counter strips. Mass resolutions for pions, protons, kaons and positrons are probably near the limit of what can be achieved with the CLAS TOF counter system. Mass resolution of about 18 MeV for pions and 22 MeV for protons have been achieved for the average particle yields at 2.445 GeV incident beam energy.

There is still room for improvements that are outside the scope of our calibration procedure. Particularly, the biggest problem that we encountered during the calibration was the double peaking in the time difference distribution for the channels from 40 to 48, which is due to the fact that these are actually two scintillator strips with separate PMTs plugged into one electronics channel. The future procedure for calibrating these channels depends on the hardware improvements such as adjusting the timing between the two strips within a single channel or assigning a separate channel to each strip.

Improvements are also needed for the time walk correction for a few channels since they give worse than overall average mass resolution. Another problem that has been noticed is that some of the channels are getting lower number of events which may cause the fitting procedure to fail, and hence it is recommended to check the quality of the fit by looking at the output plots, and in case of a failure to correct it manually.

The calibrations are going to be redone again when there is a significant improvement in the momentum reconstruction using tracking code, since the precision of our procedure depends on the path length of electrons and pions and on the momentum of pions. We believe that the systematic uncertainties in the momentum reconstruction are currently the major limitation for particle identification in the CLAS detector.

References

- [1] (see: CALCOM minutes January 16, 1998, and January 23, 1998, available at: <http://www.jlab.org/Hall-B/equipment/technical/calcom.html>)
- [2] <http://www.jlab.org/anciant>
- [3] CLAS note: 96-004, and private communications with Elton Smith and Simon Taylor.